ELSEVIER

Nuclear Instruments and Methods in Physics Research B 192 (2002) 90–96

NIM B
Beam Interactions with Materials & Atoms

www.elsevier.com/locate/nimb

Positron trapping and the creation of high-quality trap-based positron beams

R.G. Greaves [a,*], C.M. Surko [b]

[a] *First Point Scientific, Inc., 5330 Derry Avenue, Suite J, Agoura Hills, CA 91301, USA*
[b] *Department of Physics, University of California, San Diego, CA 92093, USA*

Abstract

This paper describes studies of positron accumulation and cooling using molecular gases. The production of high-quality, bright positron beams from trapped positron plasmas is also discussed. Trapping efficiency and cooling-rate measurements are presented for a number of gases. Results are presented for the radial compression of magnetized positron plasmas using a rotating electric field and molecular gas cooling. A technique to exploit plasma space-charge effects to extract the central portion of trapped plasmas is also described. The use of both techniques to produce bright positron beams in new regimes of parameter space is discussed. © 2002 Elsevier Science B.V. All rights reserved.

1. Introduction

Penning traps have been used for some time for pulse stretching applications on LINAC positron sources [1,2]. The capabilities of trap-based positron beams were considerably enhanced by the ability to accumulate large numbers of positrons from radioactive sources and to cool them to room temperature by collisions with a buffer gas [3,4]. These large collections of positrons have significant space charge and are in a well-defined plasma state, thus permitting the use of a range of techniques developed for manipulating other types of non-neutral plasmas. These techniques offer a qualitatively new method for positron beam formation and manipulation that potentially has significant advantages in efficiency, flexibility, and cost over current beam conditioning techniques.

One unique capability of trap-based beams is the ability to produce the ultra-cold positron beams [5] that are now being used for groundbreaking studies of positron–molecule interactions [6,7]. A second important capability is the production of the types of ultrashort pulses required for positron annihilation lifetime spectroscopy and time-of-flight techniques. A third important capability is brightness enhancement by radial compression of the positron plasma by applying a rotating electric field [8,9]. This effect can be further enhanced by advanced techniques for extracting the positrons from the trap, which take advantage of the positron space charge.

In this paper we discuss recent developments in positron trapping, including investigation of different gases for trapping and cooling. We also discuss brightness enhancement by plasma compression and extraction from the magnetic field of the trap.

* Corresponding author.
E-mail address: greaves@firstpsi.com (R.G. Greaves).

0168-583X/02/$ - see front matter
PII: S0168-583X(02)00717-6

2. Positron trapping and cooling

Various methods have been demonstrated for accumulating positrons from a radioactive source in Penning traps including trapping using collisions with trapped ions [10,11] and neutral gas [12]; stochastic orbits [13]; in a magnetic mirror configuration [14]; electronic damping [15] and field ionization of Rydberg positronium atoms [16]. Positron pulses from LINAC sources have also been captured in Penning traps for beam conditioning by rapid switching of the potentials on confining electrodes [1,2].

The method considered here is the buffer gas technique, which is the only method thus far demonstrated to have a high enough efficiency for high-throughput applications. The basic trapping scheme is illustrated in Fig. 1. Positrons from a neon-moderated radioactive source [17] are guided by a magnetic field into a modified Penning–Malmberg trap. The magnetic field at the source is about a factor of six less than the field of the trap, so some magnetic compression of the incoming beam (i.e. a factor of $\sqrt{6}$) is obtained. The positrons pass through a high pressure region ('I' in Fig. 1) created by continuously feeding a buffer gas into that part of the trap. In this region, the positrons are trapped by inelastic collisions, 'A', with buffer gas molecules. The positrons then filter to lower energy by collisions 'B' and 'C' and as a result are confined in region 'III', which is maintained at a low pressure by differential pumping. The pressures in the trap are such that transition 'B' takes less than 100 μs, and transition 'C' takes a few milliseconds. For optimal trapping efficiency, the electrode potentials are adjusted so that the cross sections for transitions 'A', 'B' and 'C' are maximized for electronic transitions of the buffer gas.

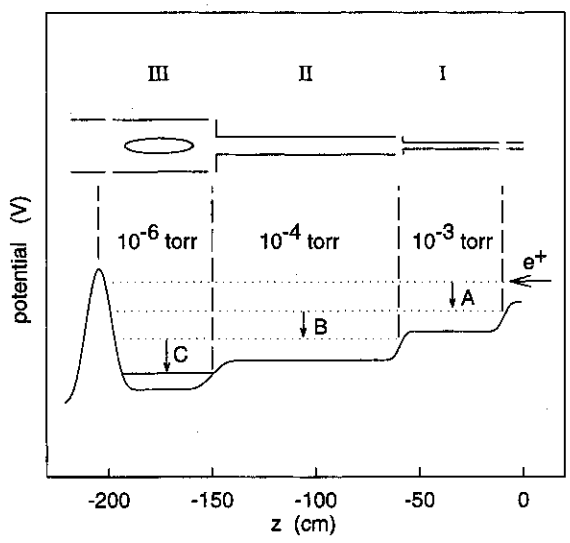

Fig. 1. Schematic diagram of a buffer gas positron accumulator, showing the three stages of differential pumping and the electrostatic potential.

In Table 1, we present a comparison of the measured trapping efficiencies for a selection of molecular gases. The data were obtained after optimizing the trapping efficiency by adjusting the electrode potentials using a computerized search procedure. As can be seen from these data, the highest trapping efficiency is obtained with N_2. High trapping efficiency can be achieved using buffer gases that have large positron-impact cross sections for electronic excitation and small positronium-formation cross sections (i.e. the dominant positron loss process in the trap). High trapping efficiency in N_2 is obtained by tuning each stage of the trap to operate at ~9–10 eV. In this case, the efficient trapping is due to electronic excitation of the $a^1\Pi$ state in N_2, which has an unexpectedly large near-threshold excitation cross section, as compared, for example to H_2 [18]. For certain applications, it may be desirable to operate a trap with another buffer gas, even though the trapping efficiency is lower. For example, the Doppler broadening of the annihilation line for

Table 1
Summary of trapping efficiencies, normalized to nitrogen for a selection of gases

Gas	Formula	Trapping efficiency (%)
Nitrogen	N_2	100
Carbon monoxide	CO	68
Oxygen	O_2	43
Sulfur dioxide	SO_2	33
Hydrogen	H_2	30
Nitrous Oxide	NO_2	20
Carbon dioxide	CO_2	16
Sulfur hexafluoride	SF_6	7
Carbonyl sulfide	OCS	4

hydrogen was measured using that gas as the buffer gas to avoid contamination of the signal from the nitrogen buffer gas. For operation of a trap at cryogenic temperatures, hydrogen is also an attractive choice, since it will not condense on the trap electrodes, except at extremely low temperatures.

Positrons cool in the third stage of the trap by a combination of vibrational and rotational excitations. The cooling rates for alternatives gases to nitrogen in the third stage have been measured. The gases studied were CO, CO_2, CF_4 and SF_6. Cooling rates were measured by filling the third stage of the trap for a time short compared to cooling times of the respective gases (~10 ms) and then releasing the positrons from the trap after a variable delay. When initially trapped, positrons have a residual energy of several volts resulting from the injection process. As the positrons cool, they develop a two-temperature distribution consisting of a low-temperature component and a high energy tail. As the cooling proceeds, positrons are transferred from the high-energy tail to the low-energy bulk by vibrational excitations of the cooling gas. By measuring the number of positrons released from the trap as a function of the exit gate potential, the positron energy distribution function can be obtained. From these data, cooling rates can be extracted. The cooling rates presented here are for vibrational cooling of the high-energy tail (e.g. at energies above 0.1–0.3 eV). It is also possible to measure cooling below the vibrational threshold using this technique if a finer energy resolution is used for the measurements, but this was not done for this experiment. However, as described below, Qaradawi et al. have made measurements in this regime using a different technique [19].

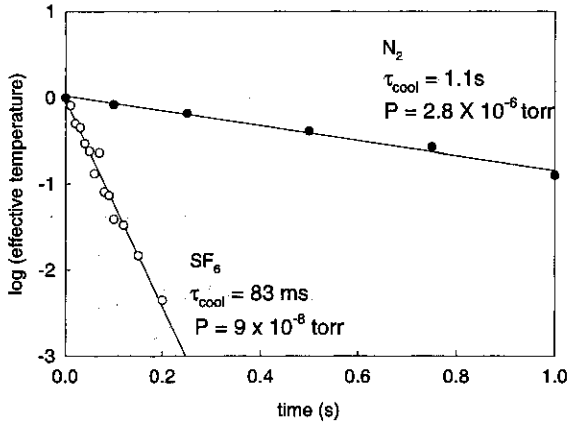

Fig. 2. Fraction of positrons in the tail of the positron energy distribution are shown as a function of time in the presence of N_2 and CF_4 buffer gases at the pressures indicated.

Typical cooling data are presented in Fig. 2. From these data a cooling rate can be extracted. The results are presented in Table 2, together with other parameters relevant to this experiment. As can be seen from these results, the cooling rates for all four of the other gases studied are dramatically larger than for nitrogen. Thus even though nitrogen is the most efficient gas for positron trapping, it is a poor choice for positron cooling. This deficiency can be overcome by introducing small quantities of a cooling gas directly into the third stage of the trap, and this has now been adopted as a standard operating procedure for the trap, using CF_4 at a pressure of $\sim 2 \times 10^{-7}$ Torr [7,18].

Table 2
Measured positron cooling times, τ_c and calculated annihilation times, τ_a, for selected molecules at a pressure of 2×10^{-8} Torr. Plasma compression rates, $\dot{n}/n$, are also shown, using the rotating electric field technique and these gases for cooling. Comparisons are also shown for cooling times measured using a qualitatively different method [19]. E_v are the vibrational energy quanta for each gas

Gas	τ_a (s)	τ_c (s)[a]	τ_c (s)[b]	E_v (eV)	$\dot{n}/n_{max}$ (s^{-1})
SF_6	2190	0.36	1.52	0.076, 0.188	10
CF_4	3500	1.2	–	0.157	10
CO_2	3500	1.3	3.8	0.291, 0.083	4
CO	2400	2.1	41	0.266	<0.2
N_2	6300	115	532	0.292	<0.2

[a] This work.
[b] Ref. [19].

Recently, cross sections have been measured for the vibrational excitation of a number of molecules (e.g. CO, CO_2 and CF_4) by low-energy positrons [6,7]. The cooling times shown in Table 2 are in reasonable agreement (e.g. to within a factor ~2), with these measurements, indicating the important role that vibrational excitation plays in buffer gas cooling.

Cooling rates for many of these gases have also been studied recently in high-density mixtures of the test gas and Ar [19]. The cooling times from that experiment are summarized in Table 2 for comparison with the present work. Except for CO, their cooling times are a factor of 3–5 longer than those reported here, reflecting the fact that the present experiment measures the initial cooling of high-energy positrons by vibrational excitation, while the data of [19] probably reflect cooling at lower energies where rotational excitations dominate. Since rotational excitations typically have lower cross sections and have smaller quanta, longer cooling times may be expected in this regime.

3. Positron compression

Positron traps have the potential for producing brightness-enhanced beam by compressing the positron plasma prior to beam extraction. This is accomplished using a method first demonstrated using pure electron plasmas [20,21]. This method involves the application of rotating electric field to a confined plasma. For this method to function efficiently, a cooling mechanism must be present. For positrons, this can be conveniently provided by the presence of a low pressure of one of the cooling gases discussed above. We now have demonstrated this technique in a proof-of-principle experiment [8,9]. The rotating electric field is generated by applying phase-shifted sine waves to an azimuthally segmented electrode surrounding the plasma. In a typical cycle, about 10–20 million positrons were accumulated in a buffer gas trap and then transferred to a separate trap where a cooling gas was introduced at a pressure of $\sim 1 \times 10^{-8}$ to $\sim 5 \times 10^{-8}$ Torr.

Following the application of the electric field, the plasma was released from the trap onto a phosphor screen biased at -10 kV and the resulting image was recorded using a CCD camera. Fig. 3(a) and (b) show typical CCD images representing the plasma in the uncompressed and compressed states, respectively. For clarity, the images are normalized to their maximum values. Fig. 3(c) shows the central density of the plasma as a function of time for a selection of applied amplitudes of the rotating field. From these data, it is clear that rapid and substantial density increases (e.g. $\dot{n}/n \sim 15\ s^{-1}$, $n_{max}/n_0 \sim 20$) can be obtained at a cooling gas pressure at which annihilation is negligible. Furthermore compression was observed over a broad range of applied frequencies, simplifying the practical implementation of the technique. This technique is now being refined and incorporated into commercial trap-based positron beam systems being developed by First Point Scientific, Inc. [22]. Much greater compression ratios are expected in these systems.

The compression technique was investigated using a selection of gases as cooling agents and the

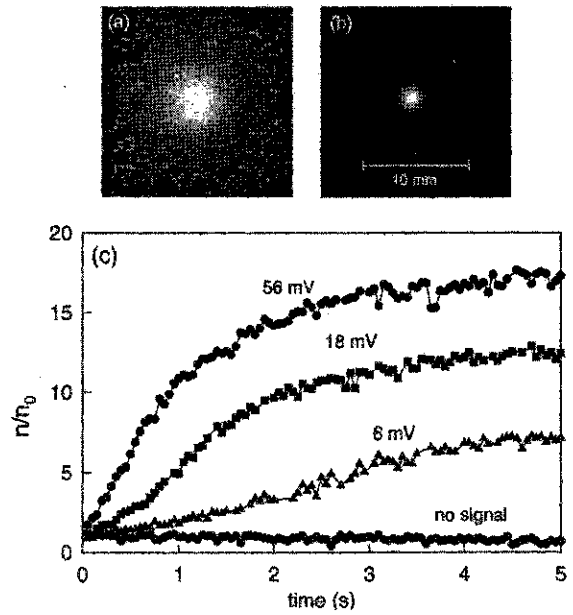

Fig. 3. CCD images of a positron plasma (a) before and (b) $t = 4$ s after the application of a rotating electric field. (c) Ratio of the central density of positron plasmas to the initial density ($t = 0$) as a function of time following the application of the rotating electric field for different amplitudes of the applied rf field.

maximum compression factors $\dot{n}/n$, obtained for each gas are summarized in Table 2. Also shown in this table are the quanta relevant for vibrational cooling. The best compression was obtained with CF_4 and SF_6, while only minimal compression was obtained with N_2 and CO. In general, there is a correlation between the cooling time and the maximum compression rate. It is interesting to note that this correlation is better for the cooling times reported in Ref. [19] than the cooling of the high-energy tail reported here, especially for the case of CO. Our interpretation is that cooling below the threshold for vibrational excitation plays an important role in the compression process.

Another technique for brightness enhancement using trapped positrons becomes possible if a significant amount of positron space charge can be accumulated in the trap. In this case, when the confining voltage is reduced to release the positrons, they are released first from the volume closest to the axis of the charge cloud. Thus, the initial beam is narrower than the charge cloud itself. This effect is illustrated in Fig. 4 using an electron plasma with a space charge of about 30 V and a temperature ~1.5 eV. As can be seen from the Figure, a significant reduction in beam diameter can be obtained using this technique.

For this technique to be effectively employed for brightness enhancement, only a small portion of the positrons should be released. The rotating electric field, in combination with natural cross-field transport processes (and perhaps instabilities occurring in the hollow plasma column) could then be used to replenish the depleted central portion of the plasma. The charge cloud would have to be continuously (or periodically) replenished to maintain the total space charge. The plasma conditions for this technique to function correctly is that the space charge potential energy must be much greater than the thermal energy of the positrons. This can be easily arranged in a positron trap because of the low positron temperature. For example, 5×10^6 positrons (amounting to only a few seconds accumulation in a buffer gas trap) in a cloud 1 cm long would have a space charge of about 1.5 V, in comparison with the thermal positron energy spread of 0.025 eV.

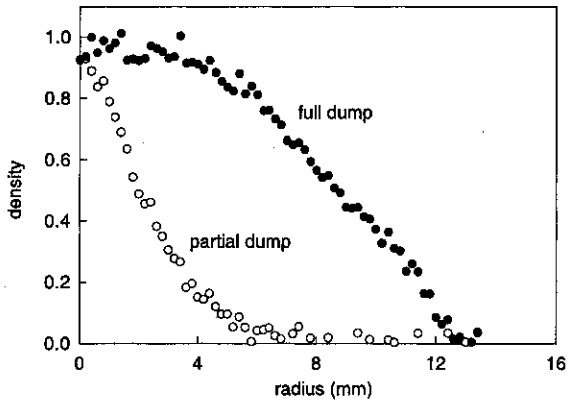

Fig. 4. Comparison between a partial release and a full release of an electron plasma with a space charge of ~30 V and a temperature of ~1.5 eV.

4. Extraction from the magnetic field

Positron beams extracted from Penning traps are magnetized because of the confining magnetic field of the trap. For many applications, it is desirable to extract the beam from the magnetic field. This leads to a degradation in the quality of the beam, because the angular momentum associated with the cyclotron motion is translated into an additional component of transverse momentum. In particular, for a beam of diameter d and transverse energy spread $\Delta E_\perp$ the beam emittance, $\varepsilon = d\sqrt{\Delta E_\perp / E_0}$, must be generalized to include a magnetic field dependent term [23]. The generalized (noninvarient) emittance is then

$$\epsilon^* \simeq d\sqrt{\frac{\Delta E_\perp}{E_0}} + \frac{ed^2B}{2^{3/2}m^{1/2}\sqrt{E_0}}, \tag{1}$$

where B is the magnetic field strength.

In Fig. 5, the generalized invarient emittance, $\sqrt{E_0}\varepsilon^*$ is plotted as a function of beam diameter for three values of magnetic field. As can be seen from this figure, the magnetic component in Eq. (1) dominates the emittance for larger diameter beams, even at magnetic fields as low as 100 G.

Various schemes have been proposed for extracting positrons from a magnetic field, all of which involve accelerating the positrons through

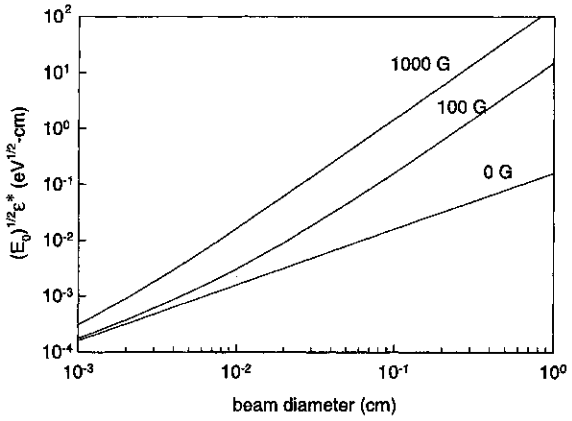

Fig. 5. Generalized emittance as a function of beam diameter for a 0.025-eV positron beam as calculated from Eq. (1).

some region in which the magnetic strength drops off rapidly [23–26]. In the most sophisticated configurations, complex magnetic terminations are used to produce abrupt changes in the magnetic field [25,26]. In others, the natural decline of the magnetic field from a small diameter solenoid is employed as a "soft" termination [24]. We have successfully used this latter method to extract positron beams from the magnetic field of a trap. The extraction geometry is illustrated in Fig. 6(a). It consists of a small diameter solenoid (4.5 cm) and a system of accelerating and focusing lenses. The extracted beam is imaged using a phosphor screen. Positrons are accelerated prior to entering the magnetic field termination and are focused by two einzel lenses following extraction. Calculated particle trajectories are shown in Fig. 6(a). These calculations show that the beam can be easily extracted and focused, but that the beam quality (as represented by the focus angle at the target) is considerably degraded for positrons starting at larger initial radii. This is expected from Eq. (1) and highlights the importance of plasma compression in obtaining high-quality beams.

Fig. 6(b) shows the beam diameter and extraction efficiency as a function of the bias voltage on electrode #5. These data indicate that extraction efficiencies as high as 90% can be obtained (keeping the spot size no larger than the original beam size) from a magnetic field as high as 450 G and a beam as large as 4.5 mm in diameter. The next

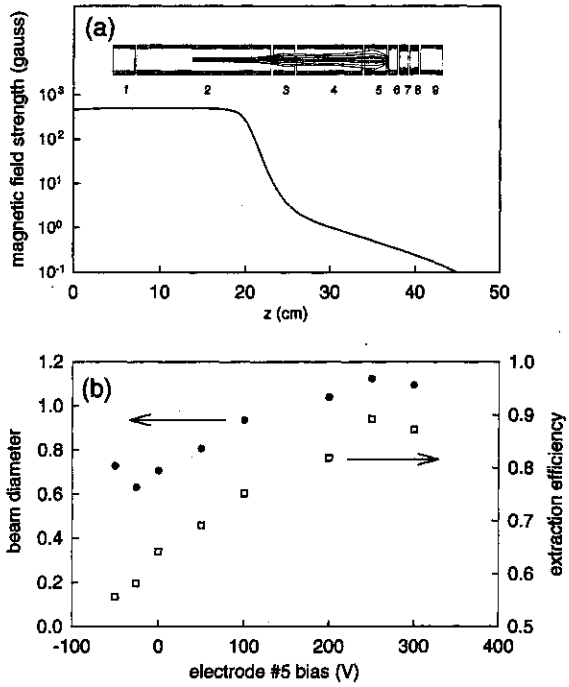

Fig. 6. (a) Electrostatic lens system for extracting positrons from a magnetic field with examples of calculated positron trajectories; and (b) measured beam diameter and extraction efficiency for a 4.5-mm diameter positron beam extracted from a 450 G magnetic field, as a function of the bias voltage on electrode #5 shown in (a). Other electrodes were biased such that $V_1 = 0$ V, $V_2 = -4$ kV, $V_3 = -200$ V, $V_4 = -30$ V and V_6–$V_9 = -4.0$ kV.

generation FPSI system will operate at a lower magnetic field (e.g. 100 G) and use the plasma compression techniques described above to obtain a significant degree of focusing, possibly even to the extent of obtaining microbeams.

5. Summary

The buffer gas positron accumulator has proven to be a relatively simple and effective way to efficiently trap and cool positron plasmas. These plasmas, in turn, provide a convenient positron source for the production of cold and/or bright positron beams. In this paper, we have described further studies of the cooling of positrons by molecular gases. We have also described techniques to

brightness-enhance positron beams, using both a rotating electric field for plasma compression and exploiting plasma space-charge effects to permit the extraction of particles from the axis of a magnetized plasma. These tools are potentially useful in a variety of applications, including study of atomic physics and establishing a quantitative antimatter–matter chemistry, the selective fragmentation of molecules including those of biological interest, the characterization of materials and material surfaces, and the study of electron–positron plasmas. The data presented here for positron cooling by specially selected polyatomic gases have, for example, already proven useful in atomic physics studies [7,18] and are crucial to the success of positron plasma compression experiments [8,9].

Acknowledgements

The work at UC, San Diego is supported by the Office of Naval Research, grant no. N000-14-97-1-0366. The work at First Point Scientific, Inc., is supported by the Office of Naval Research, grant no. N00014-00-C-0710 and the National Science Foundation, grant no. DMI-0078468.

References

[1] T. Akahane et al., Appl. Phys. A 51 (1990) 146.
[2] D. Segers, J. Paridaens, M. Dorikens, L. Dorikens-Vanpraet, Nucl. Instr. and Meth. A 337 (1994) 246.
[3] C.M. Surko, M. Leventhal, A. Passner, Phys. Rev. Lett. 62 (1989) 901.
[4] R.G. Greaves, C.M. Surko, Phys. Plasmas 4 (1997) 1528.
[5] S.J. Gilbert, C. Kurz, R.G. Greaves, C.M. Surko, Appl. Phys. Lett. 70 (1997) 1944.
[6] S.J. Gilbert, R.G. Greaves, C.M. Surko, Phys. Rev. Lett. 82 (1999) 5032.
[7] J. Sullivan, S.J. Gilbert, C.M. Surko, Phys. Rev. Lett. 86 (2001) 1494.
[8] R.G. Greaves, C.M. Surko, Phys. Rev. Lett. 85 (2000) 1883.
[9] R.G. Greaves, C.M. Surko, Phys. Plasmas 8 (2001) 1879.
[10] D.J. Wineland, C.S. Weimer, J.J. Bollinger, Hyperfine Interact. 76 (1993) 115.
[11] A.S. Newbury, B.M. Jelenkovic, J.J. Bollinger, D.J. Wineland, Phys. Rev. A 62 (2000) 023405.
[12] C.M. Surko, A. Passner, M. Leventhal, F.J. Wysocki, Phys. Rev. Lett. 61 (1988) 1831.
[13] B. Ghaffari, R.S. Conti, Phys. Rev. Lett. 75 (1995) 3118.
[14] H. Boehmer, M. Adams, N. Rynn, Phys. Plasmas 2 (1995) 4369.
[15] L. Haarsma, K. Abdullah, G. Gabrielse, Phys. Rev. Lett. 75 (1995) 806.
[16] J. Estrada et al., Phys. Rev. Lett. 84 (2000) 859.
[17] A.P. Mills Jr., E.M. Gullikson, Appl. Phys. Lett. 49 (1986) 1121.
[18] J. Sullivan et al., Phys. Rev. Lett. 87 (2001) 073201.
[19] I. Al-Qaradawi, M. Charlton, I. Borozan, R. Whithead, J. Phys. B 33 (2000) 2725.
[20] F. Anderegg, E.M. Hollmann, C.F. Driscoll, Phys. Rev. Lett. 81 (1998) 4875.
[21] E. Hollmann, F. Anderegg, C.F. Driscoll, Phys. Plasmas 7 (2000) 2776.
[22] R.G. Greaves, C.M. Surko, in: J.J. Bollinger, R.L. Spencer, R.C. Davidson (Eds.), Non-Neutral Plasma Physics III, AIP Conference Proceedings No. 498, AIP, Melville, New York, 1999, p. 19.
[23] F.J. Mulligan, M.S. Lubell, Measurement Sci. Tech. 4 (1993) 197.
[24] O. Sueoka, M. Yamazaki, Y. Ito, Jpn. J. Appl. Phys. Lett. 28 (1989) 1663.
[25] D. Gerola, W.B. Waeber, M. Shi, S.J. Wang, Rev. Sci. Instr. 66 (1995) 3819.
[26] M. Shi, D. Gerola, W.B. Waeber, U. Zimmermann, Appl. Surf. Sci. 85 (1995) 143.